Transactions, SMiRT-23
Manchester, United Kingdom - August 10-14, 2015
Division II, Paper 664, Fracture Mechanics and Structural Integrity

An experimental study on the Joule-Thomson cooling effect on metal temperatures in the vicinity of a leaking through-wall crack in a pressure vessel

Heong Wah Ng[1] and Gang Ai[2]

[1] School of Mechanical and Aerospace Engineering, Nanyang Technological University, 50 Nanyang Avenue, Singapore 639798
[2] School of Aerospace Engineering, Tsinghua University, China 100084

ABSTRACT

The Joule-Thomson effect (henceforth refer to as JT effect) is the temperature change of a gas or liquid when it is forced through a valve or porous plug (also known as throttling process). This investigation was initiated by the compressed natural gas (CNG) transportation industry to determine the extent of cooling due to leakage and its influence on the fracture toughness of material and hence its resistance to further crack extension. An experimental investigation was conducted to measure the metal temperature in the vicinity of the crack whereby argon gas was allowed to leak through a crack in a low carbon steel test plate. An experimental cylindrical pressure vessel with one end covered by a flat flange plate containing a through-thickness crack was fabricated. In order to achieve a realistic and natural appearing crack, the artificial crack was made by a liquid nitrogen cracking process. An array of thermocouples attached on the both sides of the test plate and close to the crack location monitored the metal temperature drop during the leakage of the gas. Results showed for a maximum pressure drop of 91 bar g through the wall, a metal temperature drop of 22.1°C was recorded at the crack face indicating a significant effect of 0.24 degrees Celsius drop per bar g of pressure. By linear extrapolation to a pressure of 250 barg, which is the standard pressure for containment of CNG, a 60 degrees Celsius drop may be estimated. Further studies are required taking into consideration the multitude of parameters such as: the pressures, storage quantities of the gas, initial temperature, wall thicknesses, thermal and mechanical properties of containment. It is necessary to determine whether intermittent unstable crack propagation can be arrested when the crack reaches a warm zone.

INTRODUCTION

The main characteristic of the Leak Before Break (LBB) safety concept is to insure the development of a small stable crack growth and leak rate, which can be safely detected by leak sensing technologies well before instability or unstable crack growth. An often ignored physical effect in high pressure systems associated with gas leakage is the Joule-Thomson (JT) effect. The Joule-Thomson effect describes the temperature change of a gas or liquid when it is forced through a valve or porous plug. At room temperature, all gases except hydrogen, helium and neon cool upon expansion by the Joule-Thomson process. Methane the main constituent of CNG when leaked through the container wall experiences also a temperature drop due to Joule-Thomson cooling. The chilling of the vessel wall in the vicinity of the crack will reduce the fracture toughness of the wall material which for steels decreases with temperature. The deterioration of material's fracture toughness may hasten the transition of previously stable crack propagation to critical status leading to rapid crack growth. It is therefore of interest to determine the significance of this effect and its impact on assumptions made in LBB assessments. LBB studies that do not take this effect into account may not be conservative.

Research on Joule-Thomson cooling effect of gas leaking through a crack is rare. Reepmeyer et al.(2006) carried out several hydraulic full scale fatigue tests in accordance with the requirements in Det Norske Veritas (DNV) rules for CNG containing pressure vessels on shipping carriers. Reepmeyer et al. stated that the low temperature in the crack tip area leads to a deterioration of the material's fracture toughness capacity. However there are uncertainties related to the tested results as the shape of the leak was unrealistically large as it was made by machining a slot that represented a crack of 150 mm in length and 5 mm wide in a pipe of diameter of 1.067m (42 inches) and wall thickness of 33.5 mm. The machined slot is too large to represent a realistic crack which affects the flow characteristics of the gas. These factors have a significant influence on the pressure loss, flow rates, surface conditions and consequently on the temperature drop. Notwithstanding the aforementioned deficiencies, Reepmeyer's tests reported a temperature drop of 88°C for a pressure of 250 bar which should have a very significant impact on the metal's fracture toughness. The tests gave a strong indication of the severity of the JT effect and it highlighted that this effect is indeed credible and worthy of a more thorough re-examination. Firstly, there is a need for the crack has to be more realistic and natural. Furthermore a more detailed temperature mapping should be carried out. Based on these concerns, this paper studies the JT cooling effect during the leakage of gas flowing through a more realistic crack with special attention on the manufacture of natural crack surface. After determining the temperature drop, further investigation is needed to study the impact of Joule-Thomson cooling effect on the integrity of the pressure vessel.

EXPERIMENTAL METHOD

The steps of the experimental investigations proceeded as follows:
(1)Selection of the gas.
(2)Fabrication of a realistic through-thickness crack on a small piece of crack specimen which is the same size as the central slot in test plate by using a liquid nitrogen cracking method;
(3)Welding of the small pieces of crack specimen into round steel plate to form a test plate with a realistic through-thickness crack;
(4)Design and fabrication of a pressure vessel
(5)Instrumentation and experimental setup
(6)Experimental procedure

Selection of gas

The Joule-Thomson coefficients of different gases were sourced from various references: Burnett (1933) Roebuck (1933,1934), Bridgeman (1929) and Perry (1935) and plotted as shown in Fig. 1. It can be seen that Argon has the maximum value of Joule-Thomson coefficient (about 0.29°C/bar). Methane and Argon have similar Joule-Thomson coefficients (Methane: 0.28°C/bar). For safety considerations, Argon is selected as a gas to be used in Joule-Thomson experiments instead of flammable Methane.

The temperature change with the pressure drop in a Joule-Thomson process is the Joule-Thomson coefficient by Perry (1984), Edminster (1984) and Ott (2000). The Joule-Thomson coefficient is given by:

$$\mu_{JT} = \left(\frac{\partial T}{\partial P}\right)_H \quad (1)$$

where μ_{JT} is Joule-Thomson coefficient, in K/Pa or °C/bar and T and P are the temperature and pressure change.

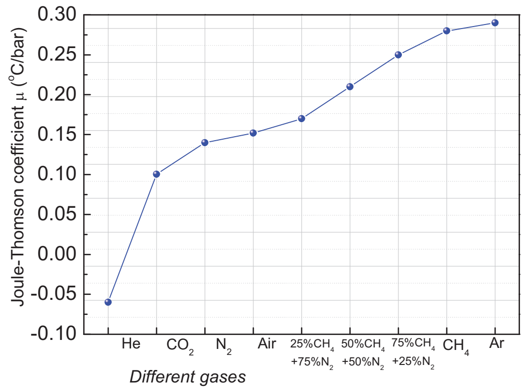

Fig. 1. Joule-Thomson coefficients of various gases

Fabrication of a realistic through-thickness crack

An illustration of the procedure of the fabrication of the test plate with a realistic through-thickness crack is shown in Fig. 2. The steps A1 to A6 show the fabrication procedure of a through-thickness crack by the liquid nitrogen cracking method via A1-A2-A3-A4-A6 (brittle fracture) and fatigue cracking method via A1-A5-A6 (fatigue fracture). Steps B1 to B3 show the fabrication process of a circular steel plate 30mm thick and diameter of 40cm with a central rectangular slot which will be clamped between the upper and lower flanges of the pressure vessel.

Firstly, a low carbon steel block with a dimension of 65×30×25 mm was machined. A 5mm deep notch was made by electrochemical wire erosion process across one face of the block as shown in Fig.3 (A1). The steel block was quenched in liquid nitrogen as shown in Fig. 3(A2). Upon the removal of the steel block from the liquid nitrogen, it was immediately placed onto the hydraulic press and under the hydraulic anvil with its notch face facing downwards as shown in Fig. 3(A3) and snapped in half. The finished steel block with realistic crack surfaces called the crack specimen is shown in Fig. 3 (A4).

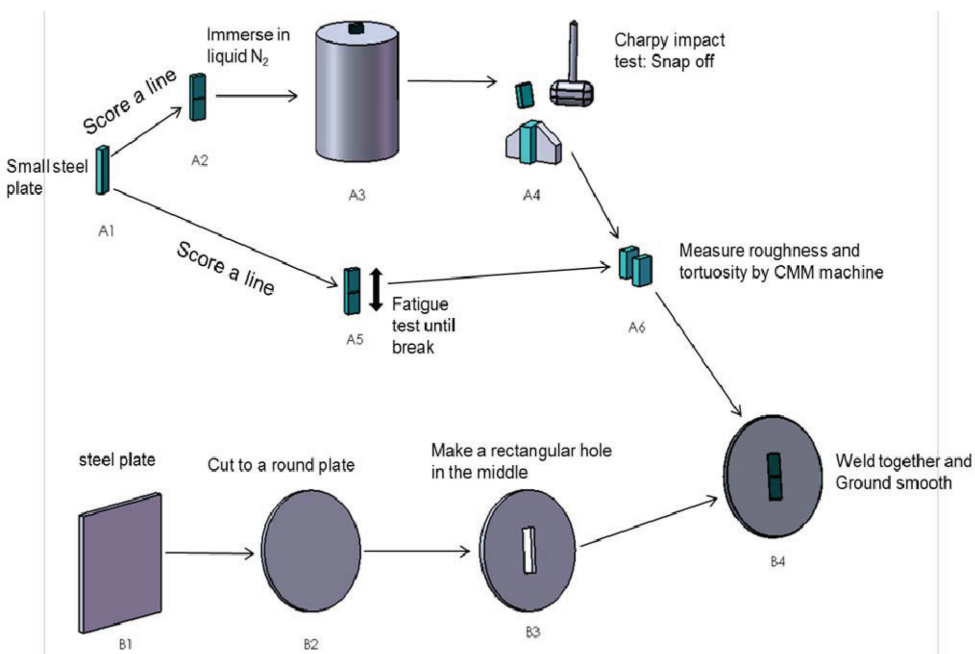

Fig. 2. Flow chart of the fabrication of test plate with a realistic through-thickness crack

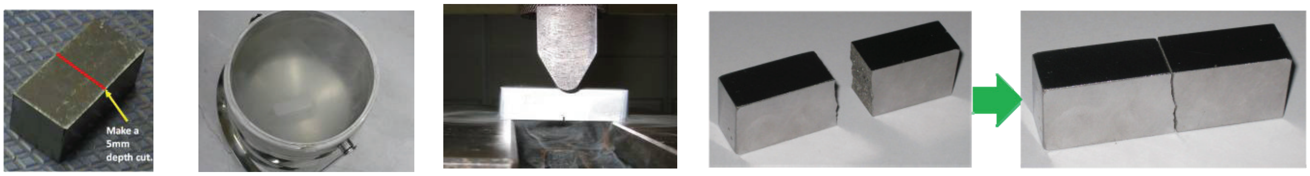

A1-Notched A2-Quenched A3-Snapped by bending A4- Reunited halves form crack specimen

Fig. 3. Steps A1 to A4 to make a crack specimen with a realistic crack

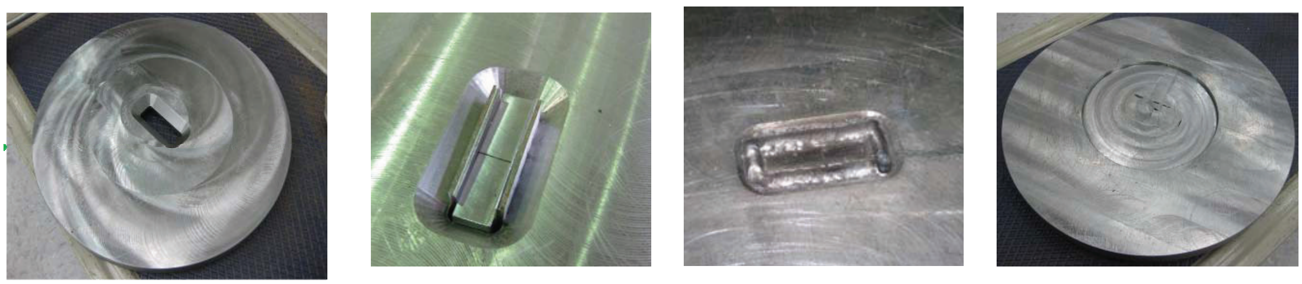

B1-B3-Plate with machined slot B4-Welding of crack specimen after inserting in slot and ground smooth

Fig. 4. Steps B1 to B4 welding the steel block to the test plate

A rectangular slot was machined at the center of the circular test plate as shown in Fig. 4 (B1 to B3). The crack specimen was inserted into the slot and welded. After welding the excess weld bead was milled flushed on both sides to remove excess weld material as shown in fig.4 B4. For the measurement of crack width, a Non-Destructive Testing (NDT) ultrasonic method was employed initially. However, after multiple attempts, it was found that the ultrasonic method gave inconclusive results. Finally, the crack width was measured by using a feeler gauge to be approximately 0.25 mm. The final size of the realistic crack is 12mm (crack length) × 0.25mm (width) × 18mm (depth) as shown in Fig. 4 B4 (last photo). The crack depth of 18mm is also the thickness of the central flat portion of the test plate.

Roughness measurement of the fracture surfaces of steel block

Surface characteristics of cracks are vitally important with regard to friction and pressure loss of flowing gas through cracks for later simulation work. Before welding the blocks together, surface roughness of the broken surfaces of steel block was measured by the TalyScan 150, manufactured by Taylor Hobson Ltd. UK. The contact method using a scanning stylus was selected to scan the broken surfaces of the steel block. The morphologies of the crack surfaces of the steel block are shown in Fig. 5. The values of root mean square Rq (RMS) in surface roughness parameters of the opposing surfaces 1 and 2 were measured to be 46.27 µm and 29.83 µm, respectively. The average roughness value of the two surfaces is 38.05 µm.

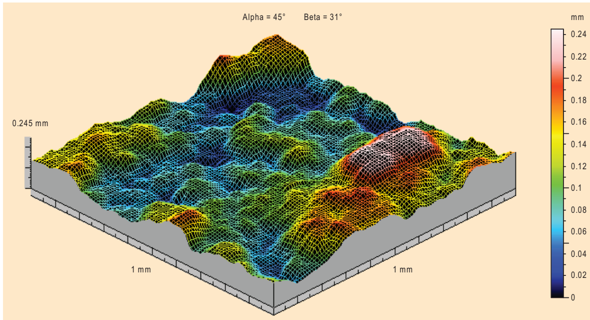

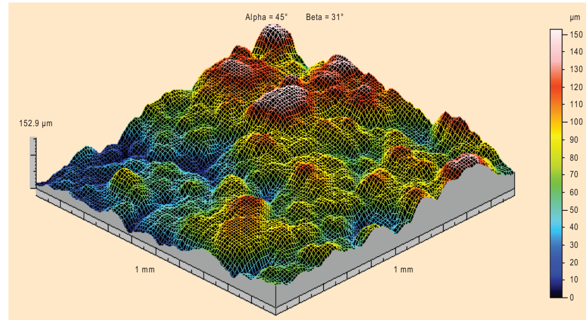

(a) Surface 1 (b)Surface 2

Fig. 5. Morphologies of broken surfaces of the steel block

Instrumentation

Thermocouples were mounted on both sides of the test plate to measure the transient metal temperature near the crack along a 3 directions with respect to the crack length, namely: along the horizontal direction (parallel to the crack line, H1 – H10), the vertical direction (perpendicular to the crack line, V1 – V10) and the diagonal direction (45° angle to the crack line, D1 – D10). The spacing of thermocouple mounting holes are shown in Fig. 6(a) and Fig. 6(b). The distances between thermocouple mounting points from the center to the edge of test plate are 3, 3, 5, 6, 6, 10, 10 and 15 mm respectively. They are closer together near to the crack to capture the temperature distributions precisely. Type K thermocouples with FEP (Fluorinated Ethylene Propylene) insulated stainless steel sheathed probes were used. The probe diameter of thermocouples is 0.32 mm. Thermocouples were calibrated to an accuracy of ±1°C. To insert the thermocouple junctions, an array of 1 mm diameter × 4 mm deep mm holes were drilled into the plate on both sides. The junctions were then inserted into the holes and pinned in to embed them in the test plate. Two thermocouple junctions were respectively placed projecting above the metal surface near the crack on both sides of the test plate to measure gas temperatures. After they were positioned on the test plate, all the thermocouple wires were neatly arranged and labelled as shown in Fig. 6(c).

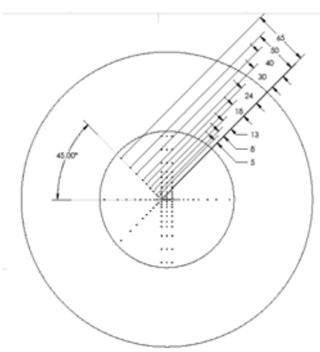

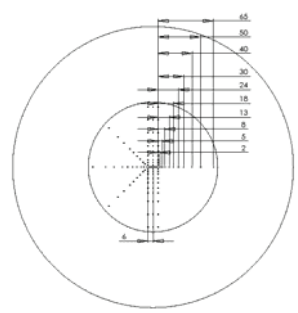

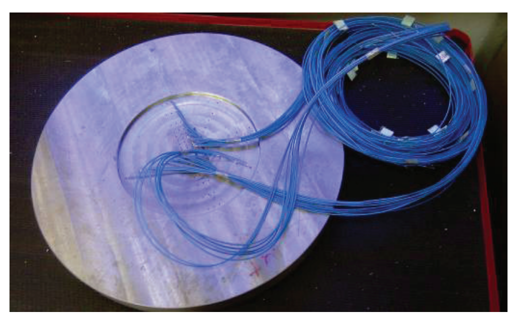

(a) Diagonal placing of thermocouples (b) horizontal placing (c)wires labelled and harnessed

Fig 6: Spacing distances of thermocouple holes and thermocouples mounted around the crack vicinity of the circular test plate.

Design and manufacture of the pressure vessel

A pressure vessel was designed to contain gas and hold the test plate such as one side of it is at a design pressure of 250 bar and the other side at external atmospheric pressure. The pressure vessel shown in Fig. 7(a). is of cylindrical design closed at one end with a hemispherical head and bolted flange with flat plate at the other end. Design dimensions were sized in accordance to ASME Boiler and Pressure Vessel Code, Section VIII, Div 2. The test plate was clamped between the upper and lower flanges by means of 12 bolts and sealed by a pair of gaskets. At the hemispherical head, a nozzle is connected through piping via a shutoff valve to the argon gas cylinders. The assembly is oriented vertically with the test plate uppermost and supported by a steel cabinet as shown in Fig. 7(b).

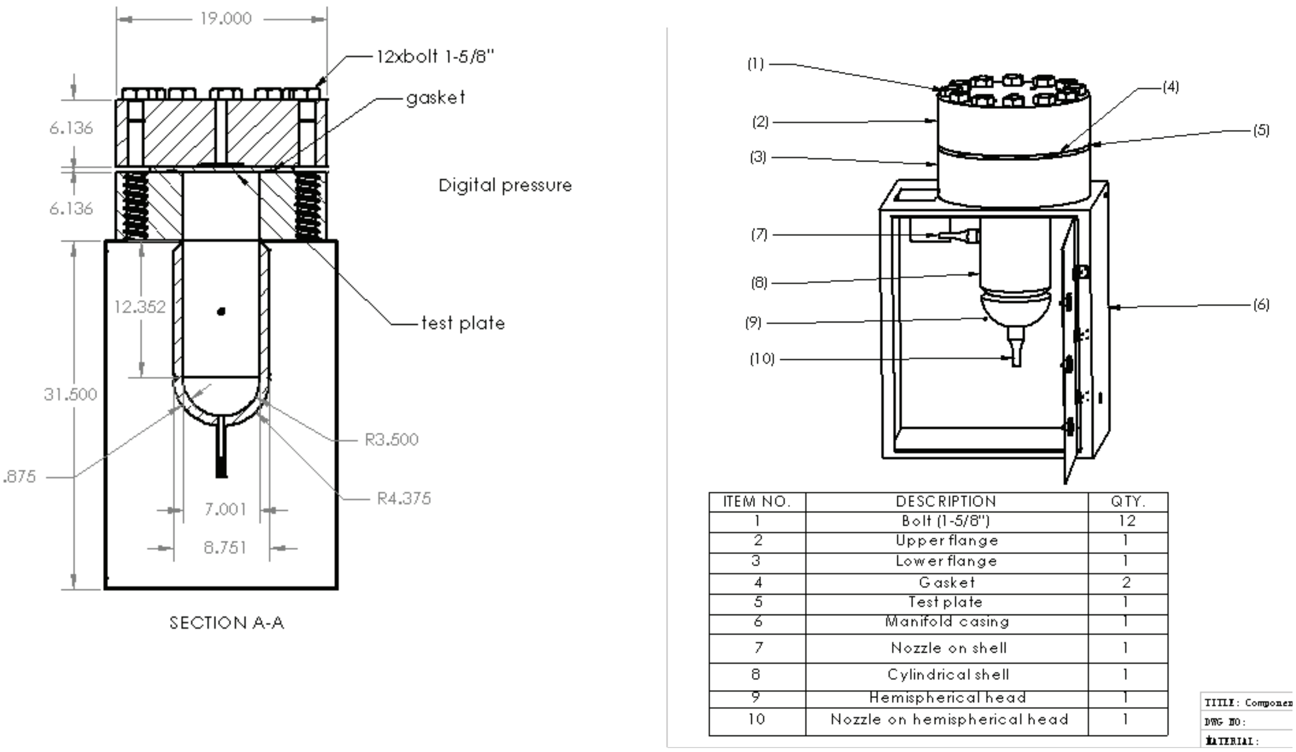

ITEM NO.	DESCRIPTION	QTY.
1	Bolt (1-5/8")	12
2	Upper flange	1
3	Lower flange	1
4	Gasket	2
5	Test plate	1
6	Manifold casing	1
7	Nozzle on shell	1
8	Cylindrical shell	1
9	Hemispherical head	1
10	Nozzle on hemispherical head	1

Fig. 7 (a) Pressure vessel dimensions and (b) support cabinet

The layout and overall arrangement of JT test rig are shown in Fig. 8 and 9 respectively. The test was conducted by tapping high pressure gas into the pressure vessel and collecting temperature data (around the crack) and pressure (inside the pressure vessel) data by using thermocouples and a pressure gauge, respectively. Thermocouple wires were bundled to go through the central hole of upper flange and connected to a data logger from which temperature data can be recorded. The digital pressure gauge with a relative accuracy of 1% connected to the side nozzle of the pressure vessel monitored and recorded the pressure inside the pressure vessel. A webcam pointing at the digital pressure gauge display monitored the pressure change and recorded via a laptop computer. The gas cylinders and the pressure vessel were located in a room which was well ventilated while the researchers are safely isolated in a nearby room with all the necessary data recording equipment. Two cylinders of Argon with a pressure of 200 bar and a purity of 99.9995 % were used for this experiment.

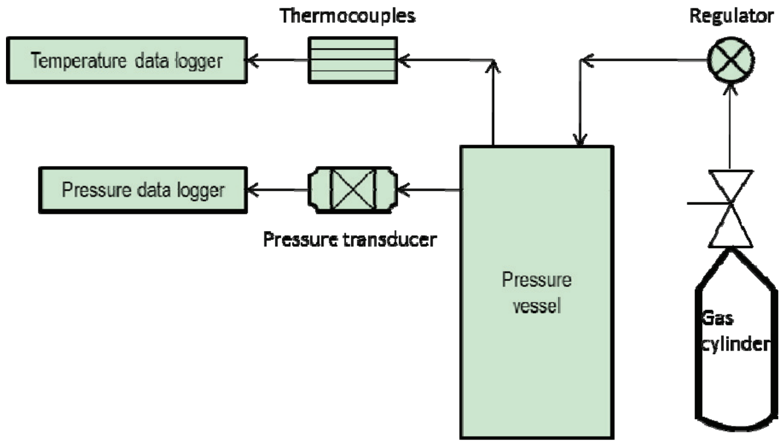

Fig 8:

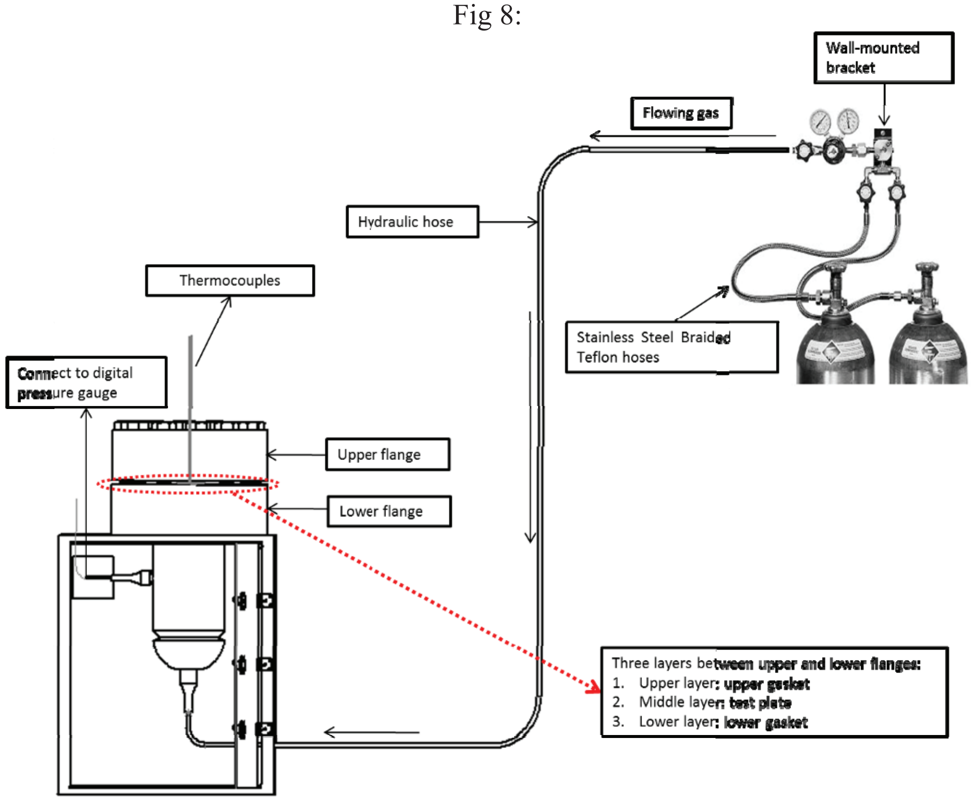

Fig 9: Layout of gas supply, sensors and control valves

Experimental procedure

During the test, the valves and regulators on the Argon gas cylinders were fully opened to pressurize the pressure vessel. Argon gas with a high pressure expanded into the pressure vessel and subsequently leaked through the crack whereby the JT effect was produced. The data of the metal temperature around the crack were recorded by data logger every few seconds. Once the temperature stabilized for a while, the vessel was depressurized by closing all the valves of gas cylinders. The temperature and pressure data were collected until the metal temperature returned to room temperature.

RESULTS AND DISCUSSION

The following parameters were recorded: t (test time), p (pressure inside the pressure vessel), T (temperature of the metal in the vicinity of the crack). The maximum pressure of Argon reached in the pressure vessel during the test is 91 bar. The temperature changes on the outside and inside surfaces of the test plate in the horizontal to the crack line are shown in Fig. 10 (a) and (b) respectively. The gas temperature were measured by thermocouples tc10. Also shown are the pressure changes referring to the left axis. From these figures, it is noted that the temperature changing trends on both inside and outside are similar during the depressurizing process.

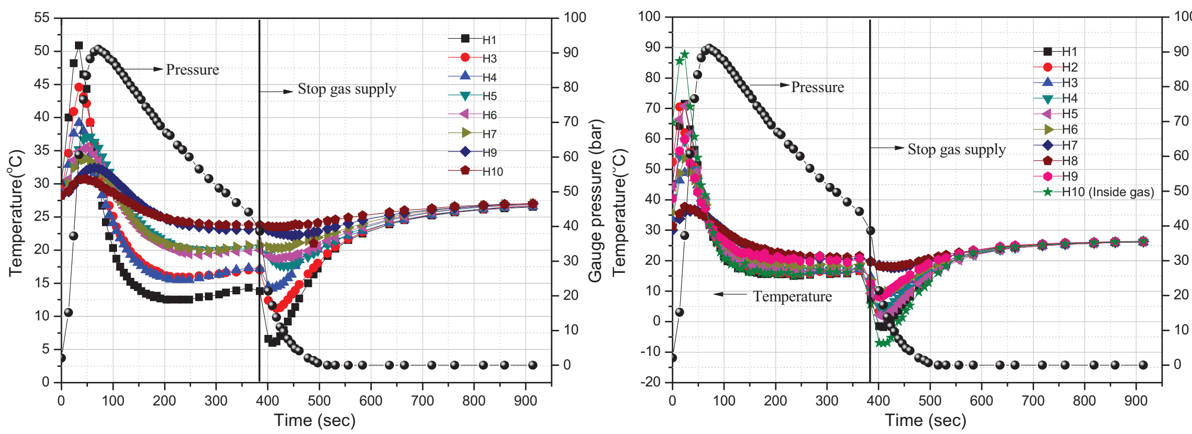

(a) Outside surface (b) Inside surface

Fig. 10. Test plate temperature (°C) and pressure (bar) changes vs. time (s) on the outside (a) and inside surfaces (b) respectively measured by thermocouples in the horizontal direction

An initial temperature rise on test plate at the beginning of the experiment was noticed which was opposite to our expectations and its cause was not initially understood but became clear later. The temperature rise phase at the beginning of the experiment was due to high pressure gas being tapped into the pressure vessel quickly while the outgoing leakage rate was negligible. This phase was the gas pressure build-up and rise in compression in the pressure vessel. The sharp increase of the gas pressure inside the pressure vessel would cause the rapid rise of gas temperature which is explained by the first law of thermodynamics. Nevertheless, the gas warming effect on the surfaces of test plate rapidly dissipated when the gas pressure inside the pressure vessel reached the maximum due to it being overwhelmed by the sharply increasing Joule-Thomson cooling effect now coming into effect. The true JT effect is measured the fall from the datum of room temperature at the beginning of the experiment and does not to include the fall from the higher warm-up phase temperature of 52°C which would exaggerate the JT effect. It is seen that the array of thermocouples show that it is a localised cooling effect, with those closest to the crack registering the largest temperature drop. The furthest thermocouples show slight drop in temperatures because the heat capacity of steel provide a large heat sink which negated the cooling. The coldest thermocouple 3mm away from the crack tip registered a drop of 22.1°C. Both inside and outside thermocouples have a similar trend, with the inside ones at lower temperature.

The Joule-Thomson cooling effect induced by the leakage begins to dominate by cooling the leaking gas shortly after the warm-up phase. The cold gas started to absorb heat from the test plate by convective and conductive heat transfer decreasing the metal temperatures. After the metal reached the lowest temperature, the temperature of the metal started to increase gradually again because the pressure in the cylinders of gas supply was already exhausted, marked by the vertical time line indicated by “stop gas supply”. At the same time, the gas pressure between the inside and the outside of the pressure vessel begin to equalised due to continuous leakage, reaching parity at 500s. Beyond 500s, there being no pressure difference to drive the gas through the crack, leakage ceased and with it the JT cooling effect. The metal temperatures begin to rise, returning to room temperature after 900s.

Clearly, the duration of the experiment is limited by the availability of the gas which was only two full cylinders of gas. It is expected that temperature will continue to fall the longer the leak is allowed to continue. It will also cause the cooled metal volume to extend outwards from the crack. Hence, a large reservoir of high pressure gases stored in large pressure vessels will prolong the duration of the leak and lead to lower temperatures. In addition, the pressure difference will be maintained to drive high leak rates with maximum cooling effect. In the case of large continuous gas pipelines, the gas source is practically infinite, pressure difference and leakage duration will be much more extended. Other factors to consider are the heat capacity of the material and initial temperature of the pressure vessel and the stored gas. It is noted from the experiment that once the leak has stopped, metal temperatures return to normal room temperature quite quickly due to the heat capacity (stored heat) of metal. The JT effect will be less severe for vessel made of metals than non metals as the greater amount of stored heat capacity in the metals will overcome the JT effect. A thick wall pressure vessel or pipe by its volume has a high heat capacity that acts as a large heat buffer. JT cooling is therefore less severe in hot climates with higher initial temperatures of both the gas and the containment to fall from than in cold climates.

It can be seen from the above test results that the maximum temperature drop of steel in the vicinity of the crack under the maximum internal pressure of 91 bar g is 22.1°C. It proves that there is a significant temperature drop of the metal around crack due to the JT cooling effect. From the materials aspect, the lower metal temperature will depress the fracture toughness of the material or the critical stress intensity factor KI_C which is temperature dependent. As JT cooling ensues, a critical juncture will be reached when KI_C falls below the prevailing stress intensity factor K of the crack front when unstable crack propagation will ensue. As already noted that the JT cooling is a localized cooling phenomena, the cooled metal volume being dependent on the reservoir capacity and other factors mentioned above. It takes a finite time to create a significant volume of material at sufficiently low temperature. In the event that unstable crack propagation initiates, it will continue propagating as the crack front stress intensity exceeds the prevailing fracture toughness of the material in its propagation path. When the crack propagates into warmer material which has higher fracture toughness, the crack will eventually arrest. Following arrest, continuous leakage will cool the freshly propagated crack front thereby lowering its fracture toughness to lead to repeated crack extension. It is therefore envisaged that the crack propagation will proceed in starts and stops with the intervening time interval for the temperature of crack front to cool to a level the prevailing fracture toughness is exceeded by the crack stress intensity. In addition, depletion of the gas and a gradual reduction of internal pressure due to leakage would lower the performance of JT cooling which eventually cause final crack arrest provided plastic collapse failure mode does not intervene first. The cycle of crack arrest and crack extension may also reduce the speed of the crack growth.

The philosophy of LBB or leak-before-break design of pressure systems lies in the technological safety barriers that detect leaks before the crack reaches a critical state to “break” uncontrollably leading to catastrophic consequences. For this to work, the maximum detectable or allowable crack size must not exceed the critical crack size (just prior to instability) by a sizable margin. That margin ensures that detection, shutdown and subsequent repair can be implemented in good time. The critical crack size as determined by the fracture toughness at room temperature or design temperature, does not take into account of Joule-Thomson cooling phenomenon. The findings of this paper showed that the low temperature reached in a leak will depress the fracture toughness, reduce the critical crack size in effect reduce the safety margin. It is therefore important that more detailed and extensive studies should be conducted to investigate the above scenarios.

CONCLUSIONS

The Joule-Thomson cooling effect was experimentally measured in a realistic crack that was made by liquid nitrogen cracking method. The advantage of nitrogen cracking method is that it produces the realistic and natural characteristic of the through-thickness crack which enables a more accurate assesment of the JT effect. In the process describe above, the brittle cracks are also easily fabricated on a small crack specimen compared to the difficult fabrication on the wall of a pipe. Due to its convenience and flexibility, the experimental method proposed in this research may provide an alternative to that of producing a through-thickness crack on a pipe wall.

This experiment proves there is a significant temperature drop of leaking argon and surrounding metal due to the Joule-Thomson cooling effect. For a maximum pressure drop of 91 bar, a most significant metal temperature drop of 22.1°C was recorded near the crack face. The lowest temperatures of the leaking argon at the outlet of the crack and nearby metal are ~9.2°C and 7.9°C, respectively. It is predicted that the resulting lower gas temperature will impact on the properties of surrounding material, especially its fracture toughness. This may bring forward the transition of previously stable crack propagation to critical leading to its rapid unstable growth and affect the validity of LBB principle. Further investigations by means of simulation and/or experiments on the leakage-induced JT cooling effect are needed to improve LBB approach.

ACKNOWLEDGEMENTS

The authors gratefully acknowledge the financial support from the American Bureau of Shipping, Singapore and the Maritime Port Authority of Singapore that have made this work possible.

REFERENCES

Bridgeman, O.C., (1929). “The Joule-Thomson effect and heat capacity at constant pressure for air”. *Physical Review*, **34**(3): p. 527-533.

Burnett, E.S., (1923). “Experimental study of the joule-thomson effect in carbon dioxide”. *Physical Review,*. **22**(6): p. 590-616.

Edmister, W.C. and B.I. Lee, (1984). *Applied Hydrocarbon Thermodynamics (2nd edition)*. Vol. 1., Oxford: Gulf Publishing.

Ott, J.B. and J. Boerio-Goates, (2000). *Chemical Thermodynamics: Principles and Applications (1st Edition)*. *Academic Press*.

Perry, J.H. and C.V. Herrmann, (1935). “The Joule-Thomson effect of methane, nitrogen, and mixtures of these gases”. *Journal of Physical Chemistry*, **39**(8): p. 1189-1195.

Perry, R.H. and D.W. Green,(1984). *Perry's Chemical Engineers' Handbook.*: McGraw-Hill Book Company.

Reepmeyer, O., et al. (2006). “Full scale gas leak test at a large diameter X-80 DSAW pipe”. in *Proceedings of the ASME International Pipeline Conference*.. Calgary, Alberta, Canada.

Roebuck, J.R. and H. Osterberg, (1934). “The Joule-Thomson effect in argon”. *Physical Review,* **46**(9): p. 785-790.

Roebuck, J.R. and H. Osterberg, (1933), “The Joule-Thomson effect in helium”. *Physical Review*, **43**(1): p. 60-69.